A Single-Inductor Current-Source-type Isolated AC-DC Converter with Active Power Decoupling for EV On-Board Chargers

Yuki Yamaguchi
Student Member, IEEE
Dept. of Electrical, Electronics and Information Engineering
Nagaoka University of Technology
Nagaoka, JAPAN
s23366@stn.nagaokaut.ac.jp

Masamichi Yamaguchi,
Student Member, IEEE
Dept. of Science of Technology Innovation
Nagaoka University of Technology
Nagaoka, JAPAN
m_yamaguchi@stn.nagaokaut.ac.jp

Kodai Nishikawa, *Member*, IEEE
Dept. of Electrical, Electronics and Information Engineering
Nagaoka University of Technology
Nagaoka, JAPAN
knishikawa@vos.nagaokaut.ac.jp

Hiroki Watanabe, *Member*, IEEE
Dept. of Electrical, Electronics and Information Engineering
Nagaoka University of Technology
Nagaoka, JAPAN
hwatanabe@vos.nagaokaut.ac.jp

Jun-ichi Itoh, *Fellow*, IEEE
Dept. of Science of Technology Innovation
Nagaoka University of Technology
Nagaoka, JAPAN
itoh@vos.nagaokaut.ac.jp

***Abstract*—This paper proposes an AC–DC converter and its control method capable of active power decoupling (APD) for electric vehicle (EV) on-board chargers. The proposed circuit reduces the component count and improves a circuit reliability because only one additional switching device and one small capacitor are required to achieve the APD. A feature of the proposed APD is a utilization of the load-side inductor to control the buffer capacitor voltage. The control methods for power factor correction, APD operation, load current regulation, and transformer magnetizing current are presented. Simulation results show the effectiveness of the proposed approach.**

Keywords—Single Inductor; Power Decoupling; AC-DC converter; On-board charger

I. INTRODUCTION

In recent years, the impact of global warming has been getting more serious, and reducing CO2 emissions has become an urgent task. One of the effective measures to reduce CO2 emissions is the electrification of power sources that utilize fossil fuels. In particular, electric vehicles (EVs) are rapidly spreading. Although EVs emit little CO2 during driving, a large amount of CO2 is emitted in the manufacturing process of on-board batteries. Thus, extending lifespan of batteries is required to reduce the production of batteries.

One of the causes of the shortens battery lifespan is power ripple during charging [1][2]. Specifically, the DC-side current in AC-DC converters connected to single-phase grids has a ripple at twice the grid frequency. Thus, power ripple reduction is necessary in on-board charger which is connected to single-phase grids. So far, electrolytic capacitors which are a large-capacitance have been widely applied to absolve power ripple in AC-DC converters. However, electrolytic capacitors are not only bulky but also short-lifespan. Thus, a power ripple reduction without electrolytic capacitors is required for single-phase grid connected on-board chargers.

On the other hand, Active Power Decoupling (APD) has been actively studied [3]-[9] as a method for reducing power ripples without the need for electrolytic capacitors. Although the APD allows applying small capacitor which are a film capacitor or a ceramic capacitor for power ripple suppression, the APD requires multiple additional devices and passive components [3][4][10]-[13].

This paper proposes an AC-DC converter and its control method, which enables APD with a small number of passive components. A feature of the proposed circuit is that only one inductor is required to achieve APD, since the load-side inductor is utilized to achieve APD. The duty ratio required for capacitor voltage control is analytically derived for proposed circuit. Finally, the validity of the proposed control based on the derived duties are verified through simulations.

II. PROPOSED CIRCUIT AND CONTROL

A. Circuit Configuration

Fig. 1 shows the proposed circuit. The proposed circuit consists of a diode bridge, an active buffer circuit [14], a full bridge, and an inductor L_o in the output stage. The output inductor L_o makes the load current I_{Load} inductive. The proposed circuit utilize the inductive load current I_{Load} to control the buffer voltage v_c of the buffer capacitor C_c for APD.

Fig. 2 shows an equivalent circuit of the proposed circuit. The secondary side circuit in the Fig. 1 is referred to the

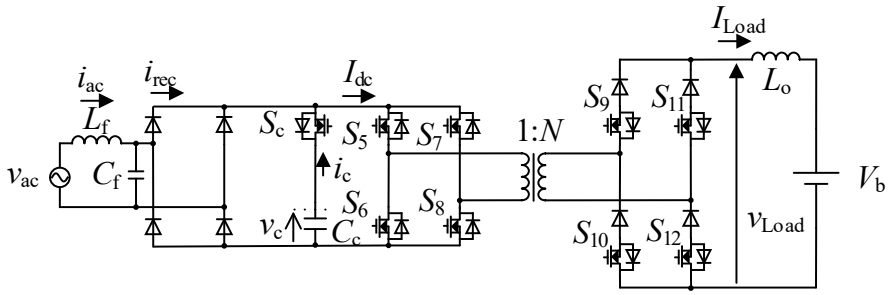

Fig. 1. Proposed circuit.

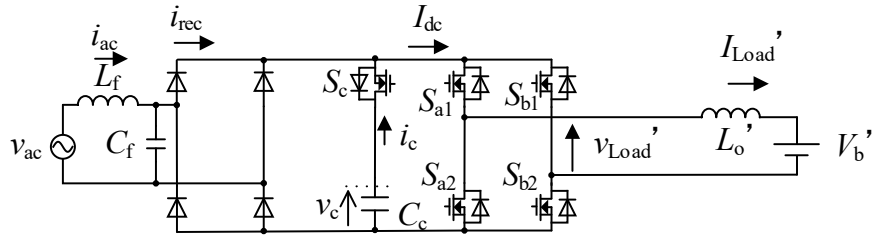

Fig. 2. Equivalent circuit of proposed circuit.

primary side and two full bridges around the transformer are omitted. The conversion formulas from the secondary side to the primary side in the equivalent circuit are given in

.....(1),

$$V_b' = V_b / N \quad \text{.....(2),}$$

$$L_o' = L_o / N^2 \quad \text{.....(3),}$$

where N is the transformer turns ratio, I_{Load} is the load current, I_{Load}' is a referred load current, V_b is the load voltage, V_b' is a referred load voltage, L_o is the output inductance, and L_o' is a referred output inductance. The control method of the proposed circuit is investigated based on the equivalent circuit shown in Fig. 2 to simplify the analysis.

B. Load Current Control

Fig. 3 shows a block diagram of load current controller in the proposed circuit. A PI controller is used to control the load current I_{Load}'. Although the output voltage v_{Load}' is the manipulated variable of the PI controller, the actual output voltage v_{Load} contains an error due to the grid voltage v_{ac} and the buffer capacitor voltage v_c. Then, the error voltage is expressed as v_{error}. Thus, the bandwidth of the PI controller is set sufficiently higher than the grid frequency and the buffer voltage frequency to suppress the output voltage error v_{error} by PI controller. Since the grid frequency is 50 Hz, the PI controller bandwidth f_c is set to 2 kHz in this paper.

C. Control Strategy for Active Power Decoupling

The APD of the proposed circuit is controlled by charging and discharging the buffer capacitor C_c using the inductive load current I_{Load}. Fig. 4 shows the charging and discharging current paths of the buffer capacitor C_c. The buffer capacitor C_c is

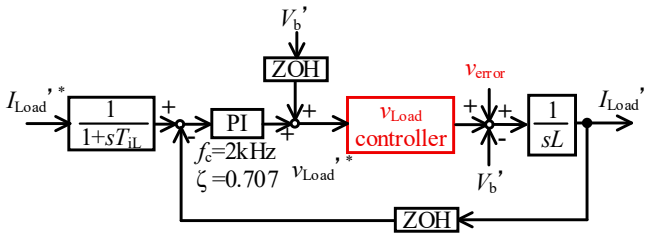

Fig. 3. Load current controller of proposed circuit.

charged and discharged via the S_c. The full bridge decides the charging mode and discharging mode by reversing the direction of I_{dc}. Fig. 5 shows a block diagram of the v_{Load} controller, which performs the APD control.

Then, the buffer voltage reference v_c^* to achieve the power decoupling is calculated by

$$v_c^* = \sqrt{V_{cave}^2 - \frac{p_{out}}{2\pi f_{ac} C_c} \sin 2\theta} \quad \text{.....(4),}$$

where V_{cave} is the average of capacitor voltage, p_{out} is the output power, f_{ac} is the grid voltage frequency, C_c is the capacitance of the buffer capacitor, and θ is the grid phase angle. The average buffer voltage is controlled by a PI controller. The Since the PI controller controls only average value, the bandwidth of the voltage PI controller is set sufficiently lower than twice the grid frequency. Thus, the bandwidth of the voltage PI controller is set to 10 Hz in this paper. On the other hand, AC component of the buffer voltage is controlled by feedforward control, which uses the buffer current command. Then, the buffer current command of the feedforward control $i_{c\_FF}^*$ is given by

$$i_{c\_FF}^* = \frac{p_{out}}{v_c} \cos 2\theta \quad \text{.....(5).}$$

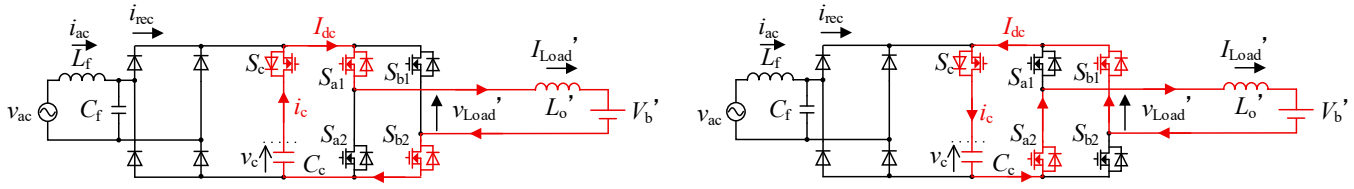

(a) Charging (b) Discharging

Fig. 4. Current flow of buffer capacitor.

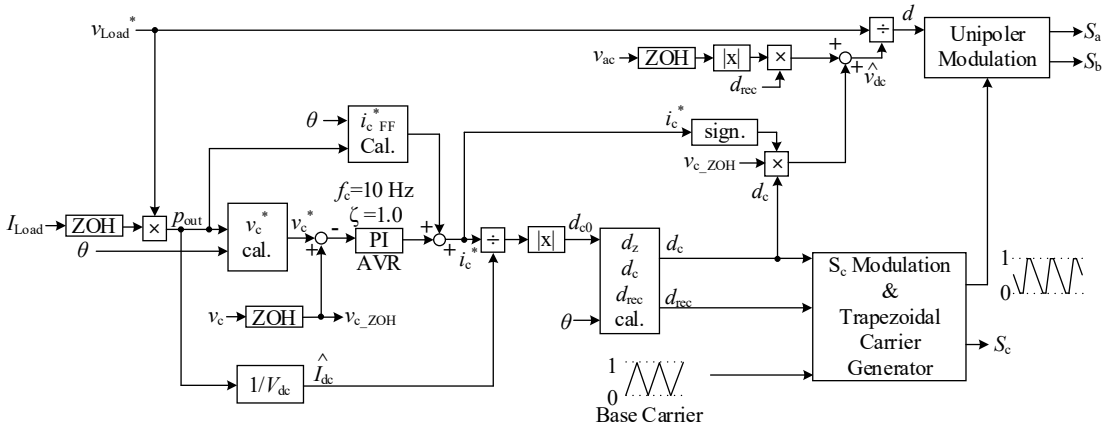

Fig. 5. v_{Load} Controller

The sum of the PI controller output and the feedforward term $i_{c\_FF}^*$ becomes the reference value of the buffer current i_c^*, which is the manipulated variable of the capacitor voltage controller. Then, each switch duty are calculated based on the capacitor current reference i_c^* by

$$d_z = 1-\left(2\alpha\gamma\left|\sin\theta\right|+d_{c0}\right) \quad \text{.....(6)},$$

$$d_c = 1-\left(2\alpha\gamma\left|\sin\theta\right|+d_z\right) \quad \text{.....(7)},$$

$$d_{rec} = 1-d_c-d_z \quad \text{.....(8)},$$

$$\begin{pmatrix} \alpha = 1-d_{zmin} \\ \gamma = \dfrac{V_{cave}}{2V_{cave}+V_{acp}} \end{pmatrix} \quad \text{.....(9)},$$

where d_c is the on-duty of S_c, d_z is the duty during the zero voltage period of the full bridge output, d_{rec} is the duty during the conduction period of the diode bridge, V_{acp} is the amplitude of the grid voltage, and d_{zmin} is the minimum value of d_z to prevent distortion of the grid current. The gate signals S_a and S_b on the equivalent circuit are generated by PWM modulation with the trapezoidal carrier and derived each duty. In addition, the gate signal of S_c is generated by comparing d_c with a triangular carrier.

D. Pulse Generation Method of Proposed Circuit

Fig. 6 shows the outlines of each carrier, switching timing of each switch, and the transformer voltage in the proposed circuit. The gate signals S_5-S_8 are generated based on the signals S_a and S_b. The transformer primary voltage is designed as a point symmetric waveform to prevent the magnetizing current saturation.

The buffer capacitor C_c is connected to the full bridge via S_c during the increasing period of trapezoidal carrier. The

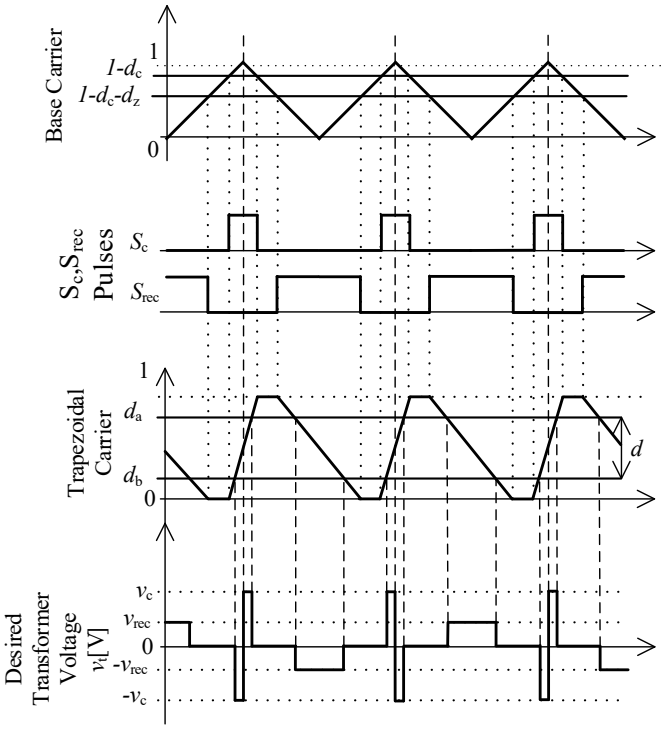

Fig. 6. Outline of modulation waveforms

output voltage is inverted by full bridge at the middle of the every on period of S_c. On the contrary, rectified grid voltage v_{rec} is supplied to the full bridge during the decreasing period of trapezoidal carrier. The output voltage is also alternated by full bridge in each decreasing period. Thus, two periods of the trapezoidal carrier are required to control the magnetizing current of the transformer. Therefore, the switching frequency

TABLE I. Conditions of Simulation

Items	Value	Items	Value
Input Voltage V_{ac}	200 V	Transformer Turn Ratio N	5.0
Input Frequency f_{ac}	50 Hz	Excitation Inductance	1.0 mH
Output Voltage V_b	400 V	Sampling Frequency f_{sample}	20 kHz
Active Buffer Capacitor C_c	195 μF	Carrier Frequency f_{sw}	100 kHz
Output Inductor L_o	1429 μH	Filter Capacitor Capacitance C_f	14 μF
Average Capacitor Voltage V_{cave}	450 V	Filter Inductor Inductance L_f	18 μH

of the proposed circuit is set as higher than two times of the sampling frequency.

III. Simulation Results

Table I shows the simulation conditions. The rated output power is 7 kW. The cutoff frequency of the input filter is designed to be 1/10 of the switching frequency. The output inductance L_o is designed based on the load current ripple.

Fig. 7 shows the simulation results of the proposed circuit. Fig. 7(a) shows that the input voltage. Fig. 7(b) shows that the input current is controlled to be sinusoidal. It indicates that the power factor of the grid side is almost unity by current control of the proposed circuit. In addition, Fig. 7(c) shows that the capacitor voltage follows the reference value. Thus, the capacitor voltage control is achieved. Moreover, Fig. 7(d) shows the current ripple suppression of the 100 Hz component of the load current. It indicates that the proposed capacitor voltage control achieves APD. The average load current is kept constant at the reference value of 17.5 A by the load current control. Its 100 Hz ripple component is 23 mA. Furthermore, Fig. 7(e) shows the transformer magnetizing current. The average value of magnetizing current is almost zero. Thus, the transformer does not become biased.

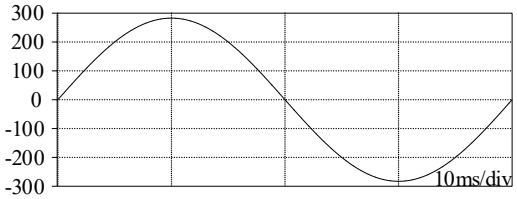

(a)AC Input voltage v_{ac}[V]

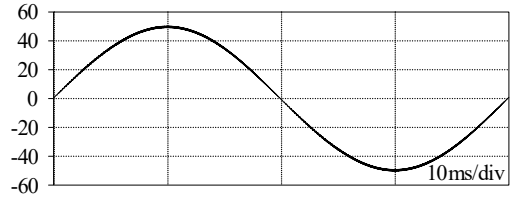

(b)AC Input current i_{ac}[A]

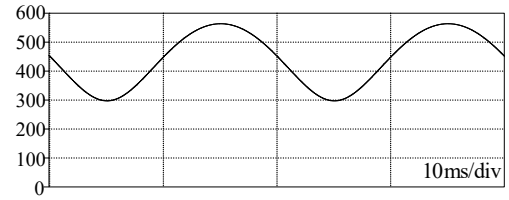

(c)Capacitor Voltage v_c[V]

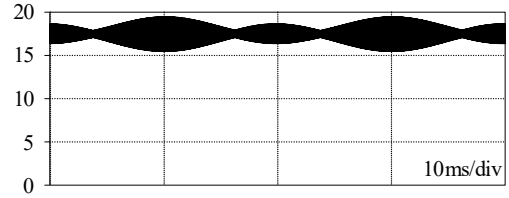

(d)Output Current I_{Load}[A]

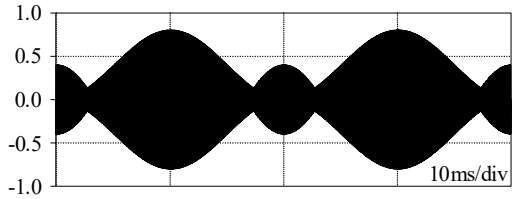

(e)Transformer Magnetizing Current[A]

Fig.7. Simulation Result.

IV. Conclusion

This paper proposed an AC-DC converter and APD control method with only one inductor. The additional components required for APD are only one switching device and one small-capacitance capacitor. The proposed circuit operations, which are load current control, power factor correction, APD operation, and transformer magnetizing current control, are verified through simulations. The 100 Hz ripple component in the load current is suppressed to 23 mA with a 195 μF capacitor for 7 kW system.

References

[1] M. Brand, M. Hofmann, and Andreas Jossen, "The influence of current ripples on the lifetime of lithium-ion batteries", *IEEE Transactions on Vehicular Technology*, Volume: 67, November 2018

[2] W. Vermeer, M. Stecca, and Pavol Bauer "A critical review on the effects of pulse charging of li-ion batteries" 2021 IEEE 19th International Power Electronics and Motion Control Conference (PEMC)

[3] Y. Sun, Y. Liu, W. Xiong, Jian Yang, "Review of active power decoupling topologies in single-phase systems" *IEEE Transactions on Power Electronics*, Volume: 31, July 2016

[4] S. Xu, L. Chang, and R. Shao, "Evolution of single-phase power converter topologies underlining power decoupling", *Chinese Journal of Electrical Engineering*, Volume: 2, June 2016

[5] Zian Qin, Yi Tang, Poh Chiang Loh, Frede Blaabjerg "Benchmark of AC and DC active power decoupling circuits for second-order harmonic mitigation in kilowatt-scale single-phase inverters", *IEEE Journal of Emerging and Selected Topics in Power Electronics*, Volume: 4, March 2016

[6] H. Li, K. Zhang, and J. Xiong "Active power decoupling for high-power single-phase PWM rectifiers", *IEEE Transactions on Power Electronics*, Volume: 28, March 2013

[7] K. Takeuchi, T. Ohno, and J. Itoh "Active power decoupling method based on dual active bridge converter without additional components", 2025 IEEE Applied Power Electronics Conference and Exposition (APEC)

[8] Y. Bi, C. Wu, and T. Soeiro "An integrated power decoupling method for single-phase EV onboard charger in V2G application", *IEEE Transactions on Power Electronics*, Volume: 38, August 2023

[9] R. Rajamony, S. Wang, and W.Ming, "Multi-objective design of single-phase differential buck inverters with active power decoupling", *IEEE Open Journal of Power Electronics*, Volume: 3

[10] Y. Tang, F, Blaabjerg, P. C. Loh, C. Jin, P. Wang, "Decoupling of fluctuating power in single-phase systems through a symmetrical half-bridge circuit", *IEEE Transactions on Power Electronics*, Volume: 30, April 2015

[11] A. Tausif, H. Jung, S. Choi "Single-stage isolated electrolytic capacitor-less EV onboard charger with power decoupling", *CPSS Transactions on Power Electronics and Applications*, Volume: 4, March 2019

[12] Y. Sun, Y. Liu, and J. Yang, "Active power decoupling method for single-phase current-source rectifier with no additional active switches", *IEEE Transactions on Power Electronics*, Volume: 31, August 2016

[13] Y. Xia, J. Roy, and R. Ayyanar, "A single stage common ground three-level PV inverter with integrated power decoupling", *IEEE Open Journal of Power Electronics*, Volume: 1

[14] Y. Ohnuma, J. Itoh "A novel single-phase buck PFC AC–DC converter with power decoupling capability using an active buffer", *IEEE Transactions on Industry Applications*, Volume: 50, May-June 2014